Inorganic Chemistry 56.19 (2017): 11810-11818

DOI: https://doi.org/10.1021/acs.inorgchem.7b01775

Group 10 metal benzene-1,2-dithiolate derivatives in synthesis of coordination polymers containing potassium countercations

Oscar Castillo,[a] Esther Delgado,[b] Carlos J. Gómez-García,[c] Diego Hernández,[b] Elisa Hernández,[b] Avelino Martín,[d] José I. Martínez[e] and Félix Zamora[b,f]**

[a]Departamento de Química Inorgánica, Universidad del País Vasco. Apartado 644, e–48080 Bilbao, Spain. [b]Departamento de Química Inorgánica, Universidad Autónoma de Madrid, 28049 Madrid, Spain. [c]Instituto de Ciencia Molecular. Universidad de Valencia. C/ Catedrático José Beltrán, 2. 46980 Paterna, Valencia, Spain. [d]Departamento de Química Inorgánica, Universidad de Alcalá. Campus Universitario, E-28871, Alcalá de Henares, Spain. [e]Departamento de Nanoestructuras, Superficies, Recubrimientos y Astrofísica Molecular. Instituto de Ciencia de Materiales de Madrid (ICMM-CSIC), 28049 Madrid, Spain. [f]Institute for Advanced Research in Chemical Sciences (IAdChem). Universidad Autónoma de Madrid, 28049 Madrid, Spain.

KEYWORDS. Coordination polymers, Metal-dithiolene polymers, Coordination compounds, First-principles calculations.

ABSTRACT. The use of theoretical calculations have allowed us to predict the coordination behavior of dithiolene $[M(SC_6H_4S)_2]^{2-}$ (M = Ni, Pd, Pt) entities giving rise to the first organometallic polymers $\{[K_2(\mu\text{-}H_2O)_2][Ni(SC_6H_4S)_2]\}_n$ and $\{[K_2(\mu\text{-}H_2O)_2(thf)]_2[K_2(\mu\text{-}H_2O)_2(thf)_2][Pd_3(SC_6H_4S)_6]\}_n$ by one-pot reactions between the corresponding d^{10} metal salts, 1,2-benzenedithiolene and KOH. The polymers are based on σ,π-interactions between potassium atoms and $[M(SC_6H_4S)_2]^{2-}$ (M = Ni, Pd) entities. In contrast, only σ-interactions are observed when the analogous platinum derivative is used instead yielding the coordination polymer $\{[K_2(\mu\text{-}thf)_2][Pt(SC_6H_4S)_2]\}_n$.

Introduction

For a long time, the chemistry of transition metals with dithiolene ligands has been high interest research field.[1, 2] Among other reasons, one of the main driving forces to focus the attention on these compounds is their outstanding electronic properties, such as magnetism and/or electrical conductivity, as well as the wide structural diversity that these compounds have shown.[3-17] However, despite many d^{10} metal-dithiolene derivatives forming discrete molecules or supramolecular networks have been widely described,[18-21] little is still known on dithiolene-based coordination polymers (CPs). Indeed, some of the examples giving rise to CPs are: $[Na(N15C5)_2]_2[M(i\text{-}mnt)_2]$ (M = Pt,[22] Pd[23]; *i*-mnt = 1,1-dicyanoethylene-2,2-dithiolate; N15C5=2,3-naphto-15-crown-5), $[K(DC18C6\text{-}A)]_2[M(mnt)_2]$,[24] (M = Ni, Pd, Pt; mnt = 1,2-dicyanoethylene-1,2-dithiolate; DC18C6-A = dicyclohexyl-18-crown-6 isomer A), $[K(DC18C6\text{-}A)]_2[Pt(i\text{-}mnt)_2]$,[25] $[\{Na(benzo\text{-}15\text{-}crown\text{-}5)\}_2Ni(i\text{-}mnt)_2]_n \cdot nCH_2Cl_2$,[26] $[\{CuL\}_2Gd(O_2NO)\{Ni(mnt)_2\}]_n \cdot CH_3OH \cdot CH_3CN$, and

$[\{CuL\}_2Sm(O_2NO)\{Ni(mnt)_2\}]_n \cdot 2CH_3CN]$ (L = N,N′-propylene-di(3-methoxysalicylideneiminato).[27]

Additionally, a microporous framework, $Cu[Ni(pdt)_2]$ (pdt_2^-=pyrazine- 2,3-dithiolate) showing electrical conductivity, doping, and redox behavior have been reported.[28] On the other hand, we have recently reported[29] on the synthesis, structural characterization, magnetic and electrical properties of 1D- or 2D-CP of $\{[K_2(\mu\text{-}H_2O)_2(\mu\text{-thf})(thf)_2][M(SC_6H_2Cl_2S)_2]\}_n$ [M = Ni, Pd], $\{[K_2(\mu\text{-}H_2O)_2(thf)_6][Pt(SC_6H_2Cl_2S)_2]\}_n$ and $\{[K_2(\mu\text{-}H_2O)(\mu\text{-thf})_2]][Pt(SC_6H_2Cl_2S)_2]\}_n$. These studies have confirmed that the presence of donor substituents in the aromatic ring of the dithiolene ligands favor the linkage of group 1 metal countercations to the group 10 metal dithiolene anionic entities by σ-interactions yielding CPs. On the other hand, some examples of organometallic polymers of alkali metals, mainly potassium, showing π-interactions to aromatic rings have been described.[30-33] However, as far as we know, compound $[K_2Fe(SC_6H_5)_4]_n$[34] is the only example of an organometallic polymer made up with transition metals aromatic thiolate entities linked by alkali complexes through σ- and π-interactions.

Our previous studies[29] confirmed the coordination of potassium centers to $[M(S_2C_6H_2Cl_2)_2]^{2-}$ ($S_2C_6H_2Cl_2$ = 1,4-dichlorobenzenedithiolate; M = Ni, Pd or Pt) entities *via* K-S and K-Cl bonds. Probably, the presence of chloride substituents in the benzene ring hampers the coordination to the aromatic carbons of this group and the formation of organometallic polymers. Herein we report how theoretical calculations may serve as a tool for the structural design of organometallic polymers based on the coordination capabilities of the $[M(SC_6H_4S)_2]^{2-}$ (SC_6H_2S = benzenedithiolate; M = Ni, Pd or Pt) entities. We also present the synthesis, characterization and physical properties of the first reported alkali metal - group 10 metal dithiolene organometallic

polymers $\{[K_2(\mu\text{-}H_2O)_2][Ni(SC_6H_4S)_2]\}_n$ (**1**) and $\{[K_2(\mu\text{-}H_2O)_2(thf)]_2[K_2(\mu\text{-}H_2O)_2(thf)_2][Pd_3(SC_6H_4S)_6]\}_n$ (**2**) as well as the coordination polymer $\{[K_2(\mu\text{-}thf)_2][Pt(SC_6H_4S)_2]\}_n$ (**3**).

Experimental

The synthesis of compounds **1**-**3** were carried out under argon atmosphere using degassed solvents. Elemental analyses were performed on an LECO CHNS-932 Elemental Analyzer.

The DC electrical conductivity was measured in the temperature range 200-400 K with the two or four contacts method (depending on the size of the crystals) on several single crystals of compounds **1**-**3**. Crystals of compounds **1**-**3** were measured in three or four consecutive scans: they were initially cooled from 300 to 200 K (since at lower temperatures the resistance was above the detection limit of our equipment, $5x10^{11}$ Ω), then heated from 200 to 400 K and then cooled again from 400 to 200 or to 300 K. The contacts were made with Pt wires (25 μm diameter) using graphite paste. The samples were measured in a Quantum Design PPMS-9 equipment connected to an external voltage source (Keithley model 2450 source-meter) and amperometer (Keithley model 6514 electrometer). Since all the crystals lose crystallinity very fast, the crystals were covered with paraffin oil immediately after the contacts where done. All the conductivity quoted values have been measured in the voltage range where the crystals are Ohmic conductors. The cooling and warming rates were 1 K min^{-1} in all cases.

Table 1. Crystallographic Data and Structure Refinement Details of Compounds **1**−**3**.

	1	**2**	**3**
formula	$C_{12}H_{12}K_2NiO_2S_4$	$C_{52}H_{68}K_6O_{10}Pd_3S_{12}$	$C_{20}H_{24}K_2O_2PtS_4$
M	453.37	1791.58	697.92
T [K]	200(2)	200(2)	200(2)
λ[Å]	0.71073	0.71073	0.71073
crystal system	monoclinic	triclinic	orthorhombic
space group	P21/n	P-1	Pnma
a [Å]	6.9977(4)	11.8802(4)	13.8768(2)
b [Å]	19.160(1)	12.2975(9)	25.1331(4)
c [Å]	7.1060(6)	14.311(2)	7.3964(3)
α [º]		101.661(8)	
β [º]	111.093(7)	98.624(6)	
γ [º]		116.546(7)	
V [$Å^3$]	888.9(1)	1761.5(3)	2579.6(1)
Z	2	1	4
ρ_{calcd} [g cm^{-3}]	1.694	1.689	1.797
μ [mm^{-1}]	2.027	1.517	6.100
F(000)	460	904	1360
reflections collected	19946	38360	23195
unique data / parameters	2037 / 97	8066 / 382	2978 / 136
R_{int}	0.118	0.068	0.094
reflections [I>2σ(I)]	1367	5612	2338
goodness of fit (S)[a]	1.296	1.122	1.070
R1[b]/wR2[c] [I>2σ(I)]	0.0568/0.1235	0.0457/0.0948	0.0448/0.0958
R1[b]/wR2[c] (all data)	0.1073/0.1522	0.0869/0.1163	0.0678/0.1110
largest diff. peak/hole [e·$Å^{-3}$]	1.265/-0.668	2.144/-1.163	2.743/-2.534

[a] $S = [\sum w(F_0^2 - F_c^2)^2 / (N_{obs} - N_{param})]^{1/2}$. [b] $R1 = \sum||F_0|-|F_c|| / \sum|F_0|$. [c] $wR2 = [\sum w(F_0^2 - F_c^2)^2 / \sum wF_0^2]^{1/2}$; $w = 1/[\sigma^2(F_0^2) + (aP)^2 + bP]$ where $P = (\max(F_0^2,0) + 2Fc^2)/3$ with a = 0.0596 (compound **1**); a = 0.0363 (compound **2**); a = 0.0419 (compound **3**);, and b = 3.5289 (compound **1**); b = 5.4711 (compound **2**); b = 16.0296 (compound **3**).

Magnetic measurements were performed with a Quantum Design MPMS-XL-5 SQUID magnetometer in the temperature range 2-300 K with a magnetic field of 0.5 T on polycrystalline samples of compounds **1**-**3**, all immersed in their mother liquor (with dry masses of 14.97, 15.64 and 19.31 mg, respectively). Susceptibility data were corrected for the sample holder and for the diamagnetic contribution of the salts using Pascal's constants.[35]

Crystal structure determination of complexes 1-3. Single crystals of compounds **1**-**3** were covered with a layer of a viscous perfluoropolyether (Fomblin®Y), mounted on a cryoloop™ with the aid of a microscope and immediately placed in the low temperature nitrogen stream of the diffractometer. The intensity data sets were collected at 200 K on a Bruker-Nonius KappaCCD diffractometer equipped with an Oxford Cryostream 700 unit. The structures were solved, by using the WINGX package,[36] by direct methods (SHELXS-2013)[37, 38] and refined by least-squares against F^2 (SHELXL-2014).[38] All the hydrogen atoms were positioned geometrically and refined by using a riding model. All the non-hydrogen atoms were refined anisotropically. Table 1 collects crystallographic data and structure refinement details of **1**−**3**.

Compound **2** presented disorder in the O5, C71, C72, C73, and C74 atoms of the tetrahydrofuran molecule. By using the corresponding Shelxl's PART commands[37-39] and FVAR variables, two positions were refined with 56 % and 44 % occupancy, respectively.

Synthesis of compound $\{[K_2(\mu\text{-}H_2O)_2][Ni(SC_6H_4S)_2]\}_n$ (1). HSC_6H_4SH (181 mg, 1.27 mmol) was added to 10 mL of a 5 % aqueous solution of KOH. Then, a solution of $NiCl_2 \cdot 6H_2O$ (150 mg, 0.63 mmol) in 10 mL of EtOH/H_2O (1:1) was slowly added. The mixture was stirred for 30 min, and then the solvent was removed under vacuum yielding a solid residue which was washed

with *n*-hexane and extracted with THF. Crystallization of the solid in wet THF/*n*-heptane (1:1) at room temperature yielded crystals suitable for X-ray analysis of compound **1** (125 mg, 43.76 %). Anal. Calcd. (Found) for $C_{12}H_{12}K_2Ni\ O_2S_4$: C, 31.79 (37.96); H, 2.67 (4.20); S: 28.29 (26.46) %.

Synthesis of compound $\{[K_2(\mu\text{-}H_2O)_2(thf)]_2[K_2(\mu\text{-}H_2O)_2(thf)_2][Pd_3(SC_6H_4S)_6]\}_n$ (2). Compound **2** has been obtained following the same procedure to prepare compound **1**, but using $Pd(OAc)_2$ as starting material and keeping the reaction for 3.5 h. Suitable crystals for X-ray diffraction analysis (257 mg, 34.9 %) were obtained by crystallization of the solid in a wet solution of THF/*n*-heptane (1:1) at room temperature. Anal. Calcd. (Found) for $C_{52}H_{68}K_6O_{10}Pd_3S_{12}$: C, 34.86 (34.51); H, 3.83 (3.81); S, 21.48 (22.26) %.

Synthesis of compound $\{[K_2(\mu\text{-}thf)_2][Pt(SC_6H_4S)_2]\}_n$ (3). Compound **3** was obtained following the same procedure as for compound **2** but using K_2PtCl_4 instead. Crystallization in wet THF/*n*-heptane (1:1) at room temperature yielded suitable crystals for X-ray diffraction of **3** (82 mg, 32.64 %). Anal. Calcd. (Found) for $C_{20}H_{24}O_2S_4PtK_2$: C, 34.42 (29.73); H, 3.47 (3.01); S, 18.38 (15.13).

Theoretical Calculations

In order to rationalize these different packing behaviors within each crystal we have carried out a set of first-principles DFT-based calculations. For that purpose we have made use of the concept of the Fukui functions $f^{\pm}(\boldsymbol{r})$[40, 41] defined as:

$$f^{\pm}(\boldsymbol{r}) = \left[\frac{\partial \rho(\boldsymbol{r})}{\partial N}\right]_v^{\pm}, \qquad (1)$$

which measure the change in the chemical potential as the number of electrons changes from N to $N+dN$ or to $N-dN$, respectively. In particular, given that the $[M(SC_6H_4S)_2]$ and $[M(SC_6H_2Cl_2S)_2]$ units will act with a net charge state of -2 within each crystal, we have used the positive Fukui function $f^+(\mathbf{r})$ to elucidate sites with enhanced reactivity within the complexes $[M(SC_6H_4S)_2]$ and $[M(SC_6H_2Cl_2S)_2]$ for M=Ni, Pd and Pt as they accommodate extra electronic charge. By construction, $f^+(\mathbf{r})$ describes the way in which the electron density $\rho(\mathbf{r})$ changes as the number of electrons in the complex increases from N to $N+dN$ (in this case from 0 for the neutral case towards the accommodation of 2 extra electrons) at constant external potential.[40, 41] This means that regions where $f^+(\mathbf{r})$ is large are able to stabilize an uptake electronic charge, and are reactive towards the anchoring electron-rich reactants nucleophiles. In practice, the two Fukui functions can be obtained using a finite difference approximation, as the density differences.[40, 41]

$$f^+(\mathbf{r}) = \rho_{v,N+1}(\mathbf{r}) - \rho_{v,N}(\mathbf{r}),$$
$$f^-(\mathbf{r}) = \rho_{v,N}(\mathbf{r}) - \rho_{v,N-1}(\mathbf{r}) \qquad (2)$$

We have computed the positive Fukui function $f^+(\mathbf{r})$ for the different isolated complexes $[M(SC_6H_4S)_2]$ and $[M(SC_6H_2Cl_2S)_2]$ with M=Ni, Pd and Pt (Figures 1, S1 and S2) based on the electronic charge densities obtained by the GAUSSIAN09 simulation package[42] within a quantum-chemistry all-electron B3LYP model accounting for cc-pVQZ basis sets for H, C, S and Cl, and LanL2DZ basis sets for M=Ni, Pd and Pt (details in Ref. 42). In all the calculations the most stable electronic spin-configuration is the low-spin (LS) state, in which all eight d electrons in the metal atom are paired ($S = 0$). This is consistent with the well-known 4-coordinate $[Ni(II)/Pd(II)/Pt(II)]S_4$ square planar complexes,[43] just the present case in both the $[M(SC_6H_4S)_2]$ and $[M(SC_6H_2Cl_2S)_2]$ configurations.

DFT-based calculations have been carried out on the different building blocks (including the K-based ligands) in two different configurations each: a) in the configuration where the two K atoms per unit cell are located one of them on a C-ring hollow site (mostly interacting with the inner C-C bridge close to the S atoms) and the other one on a S-S bridge of the $[M(SC_6H_4S)_2]$ units; and b) in the configuration where both K atoms are located on each S-S available bridges (Figure S3). Some of these computed geometries have not been detected in the experiments (configurations in right column of Figure S3), which have been heuristically constructed "by hand" as a proof-of-concept to be directly compared with the experimentally evidenced ones. We have performed full geometrical optimization to minimize the net forces acting on each atom (below 0.1 eV $Å^{-1}$). These calculations have been carried out by the efficient plane-wave code QUANTUM ESPRESSO.[44] The exchange-correlation (XC) effects have been accounted for by using the revised version of the generalized gradient corrected approximation (GGA) of Perdew, Burke, and Ernzerhof (rPBE),[45] and RRKJ norm-conserving scalar-relativistic pseudopotentials have been considered to model the ion-electron interaction.[46] In these calculations, the Brillouin zones (BZ) were sampled by means of optimal Monkhorst-Pack grids[47] guaranteeing a full convergence in energy and electronic density. A perturbative van der Waals (vdW) correction was used to account long-range interaction and checking the reliability of all the structures.[48, 49]

Results and Discussion

First-principles DFT-computed positive Fukui function $f^{+}(r)$ has been used to elucidate sites with enhanced reactivity within $[M(SC_6H_4S)_2]$ or $[M(SC_6H_2Cl_2S)_2]$ (M = Ni, Pd or Pt) entities as they accommodate extra electronic charge (up to -2; net charge state with which they act within each crystal). Figures 1 and S1 provides 3D isosurfaces of $[M(SC_6H_4S)_2]^{2-}$ and $[M(SC_6H_2Cl_2S)_2]^{2-}$

, respectively, corresponding to the Fukui function $f^{+}(\boldsymbol{r})$ for the different complexes (all with a

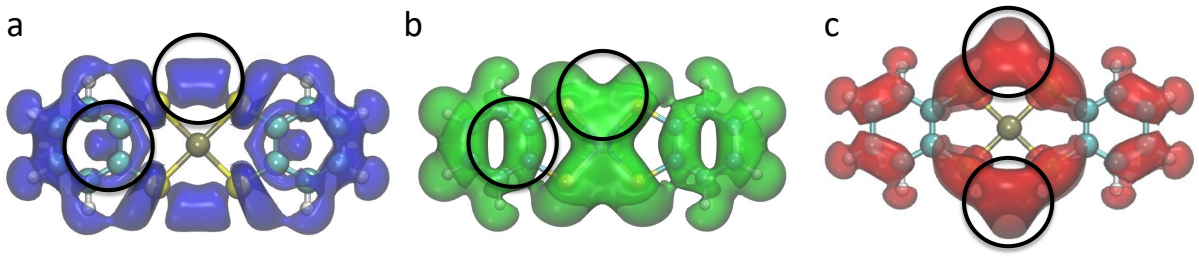

Figure 1. Computed 3D isosurfaces corresponding to the positive Fukui function $f^{+}(\boldsymbol{r})$ for the different isolated $[M(SC_6H_4S)_2]^{2-}$ entities [a) M = Ni, b) M = Pd, and c) M = Pt]. All the 3D isosurfaces are shown for a value of +0.0005 e^{-} $Å^{-3}$. Superimposed black circles indicate the most favorable sites to anchor metal centers per unit cell according to the largest value regions of $f^{+}(\boldsymbol{r})$.

value of +0.0005 e^{-} $Å^{-3}$). The $f^{+}(\boldsymbol{r})$ isosurfaces for $[M(SC_6H_2Cl_2S)_2]^{2-}$ (M = Ni, Pd or Pt) show the preferential donor sites located at the S and Cl atoms, while the C-rings are almost deactivated therefore precluding any metal coordination (Figure S1). This is in agreement with our reported experimental observations.[29] Analogous calculations carried out on $[M(SC_6H_4S)_2]^{2-}$ show that for the $[Ni(SC_6H_4S)_2]^{2-}$ and $[Pd(SC_6H_4S)_2]^{2-}$ entities (Figure 1a-b) the most favorable position to accommodate the excess of electronic charge and coordinate to metal atoms are on the C-rings, close to the inner C-C bond, and on a S-S bridge. In contrast, for $[Pt(SC_6H_4S)_2]^{2-}$ the most favorable position is centered at the two S-S bridges (Figure 1c). Importantly, for $[Ni(SC_6H_4S)_2]^{2-}$ and $[Pd(SC_6H_4S)_2]^{2-}$ $f^{+}(\boldsymbol{r})$ adopts large values simultaneously by symmetry in both S-S bridges with the possibility to coordinate metal atoms on them. Therefore, these findings indicate that in the case of $[Ni(SC_6H_4S)_2]^{2-}$ and $[Pd(SC_6H_4S)_2]^{2-}$ the carbon atoms of the

aromatic rings are not deactivated, suggesting the possibility to form metalorganic polymers by coordination of metal centers to sulfur and/or to the benzene ring.

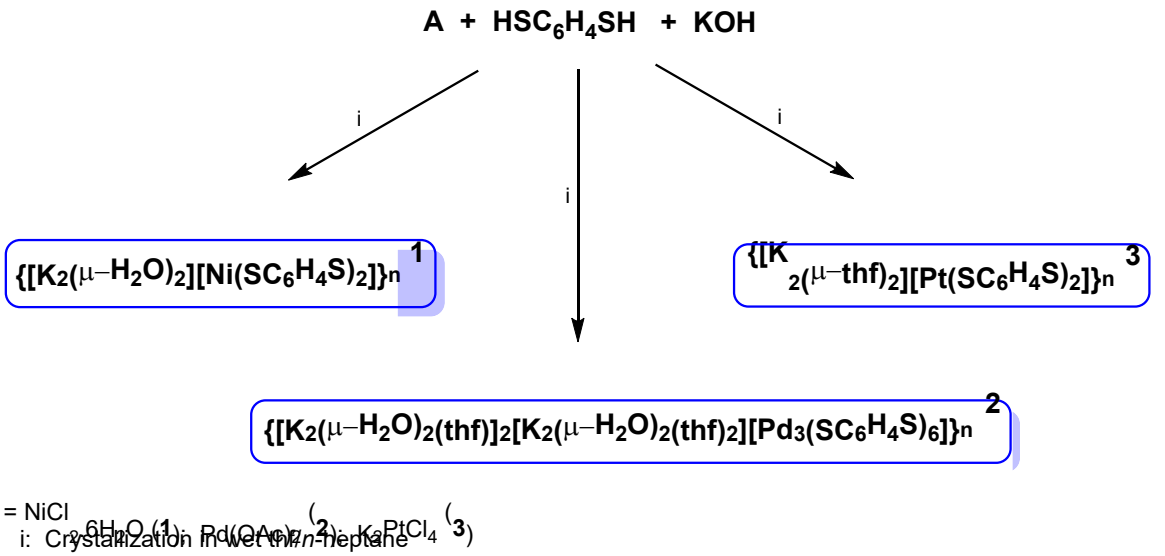

Scheme 1. Schematic representation of the reactions carried out to synthetize compounds **1-3**.

These results prompted us to evaluate the coordination of potassium ions to $[M(SC_6H_4S)_2]^{2-}$ (M = Ni, Pd or Pt). Thus, compounds **1-3** have been prepared, under argon atmosphere, by addition of a EtOH/H_2O solution of $NiCl_2·6H_2O$, $Pd(OAc)_2$ or K_2PtCl_4 to an aqueous solution of HSC_6H_4SH and KOH and further crystallization in wet THF/n-heptane (Scheme 1).

Compounds **1-3** are built-up from nearly planar $[M(\kappa\text{-}S,S'\text{-}SC_6H_4S)_2]^{2-}$ entities [M^{II} = Ni (**1**), Pd (**2**), Pt (**3**); SC_6H_4S = benzene-1,2-dithiolate] and potassium counterions to balance the charge. The nature of the group 10 metal in the dithiolate entities seems to determine the potassium coordination environment (Figure 2).

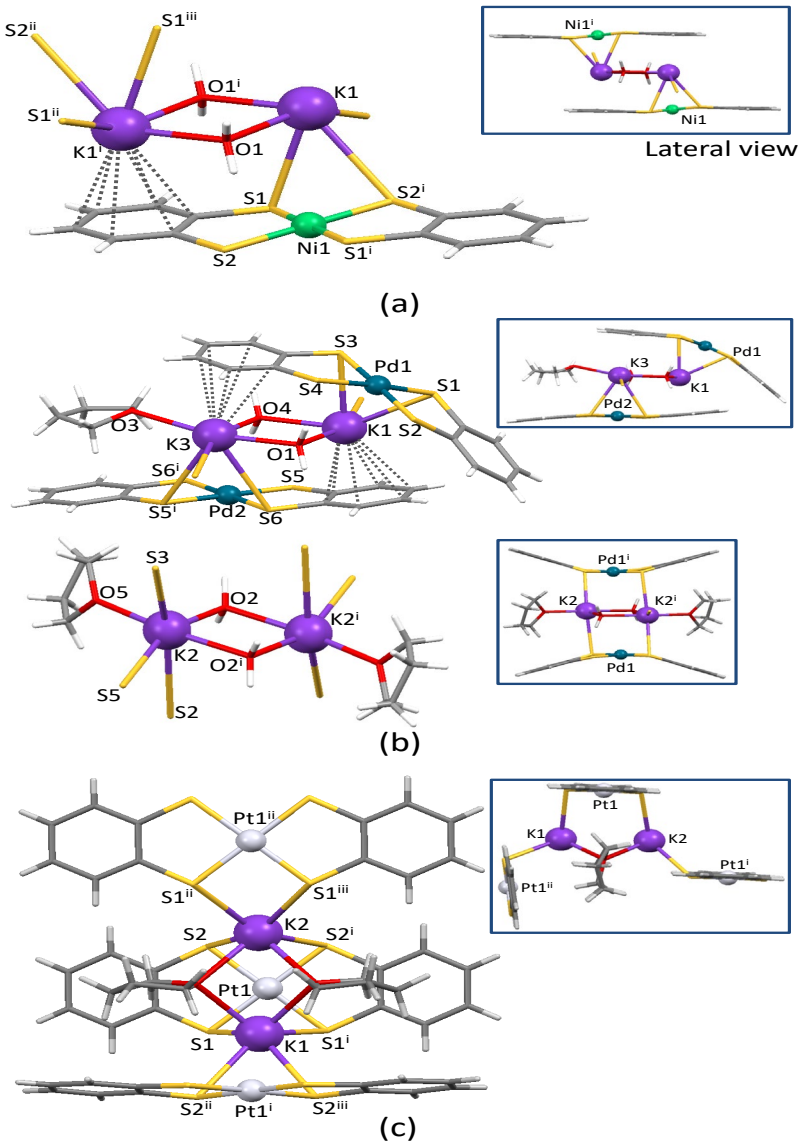

Figure 2. Details of the potassium coordination environments in compounds **1** (a), **2** (b) and **3** (c).

The crystal structure of compound **1** consists of almost planar $[Ni(SC_6H_4S)_2]^{2-}$ entities, acting as metalloligands towards $[K_2(\mu\text{-}OH_2)_2]^{2+}$ dinuclear moieties through the sulfur atoms and the benzene ring of the dithiolene, to form neutral sheets (Figure 2a). The mean plane of the benzene-1,2-dihiolate ligands coordinated to the metal center are parallel but slightly displaced 0.5 Å and present a dihedral angle of 9.6° with respect to the strictly planar NiS_4 core. The

coordination sphere of the potassium cation is completed by three sulfur atoms from two $[Ni(SC_6H_4S)_2]^{2-}$ entities (K-S: 3.32-3.46 Å), two bridging water molecules (K-O: 2.71-2.76 Å) and the η^6-coordinated benzene ring (K-C: 3.40-3.47 Å) from a third $[Ni(SC_6H_4S)_2]^{2-}$ entity in a distorted octahedral arrangement. Therefore, the benzene-1,2-dithiolate ligands adopts a chelating mode towards nickel but they also coordinate to potassium atoms in such a way that every sulfur atom establishes 2 (1Ni + 1K) or 3 (1Ni + 2K) coordination bonds. All the Ni-S and K-O distances are within the range usually found in the literature (Table 2). The internal cohesion of the sheet is reinforced by O-H···S hydrogen bonds involving the water molecules. Finally, these sheets are held together by means of edge to face interactions among these benzene rings located at both sides of the Ni/K/S/water central core Figure 3.

Table 2. Selected coordination bond lengths (Å) for compound **1**.

Ni1–S1 x 2	2.1778(13)	K1-O1	2.757(5)
Ni1–S2 x 2	2.1708(13)	K1–O1^{i}	1.970(2)
		K1–S1^{i}	1.985(2)
		K1-S1^{ii}	3.3172(19)
		K1-S2^{iii}	3.4624(19)
		K1-C1	3.459(5)
		K1-C2	3.468(5)
		K1-C3	3.421(6)
		K1-C4	3.401(6)
		K1-C5	3.421(7)
		K1-C6	3.435(6)
Ni1···K1^{iv}	3.7098(14)		

Symmetry codes: (i) –x+1, -y+2, -z+1; (ii) x, y, z-1; (iii) x+1, y, z+1; (iv) x-1, y, z-1.

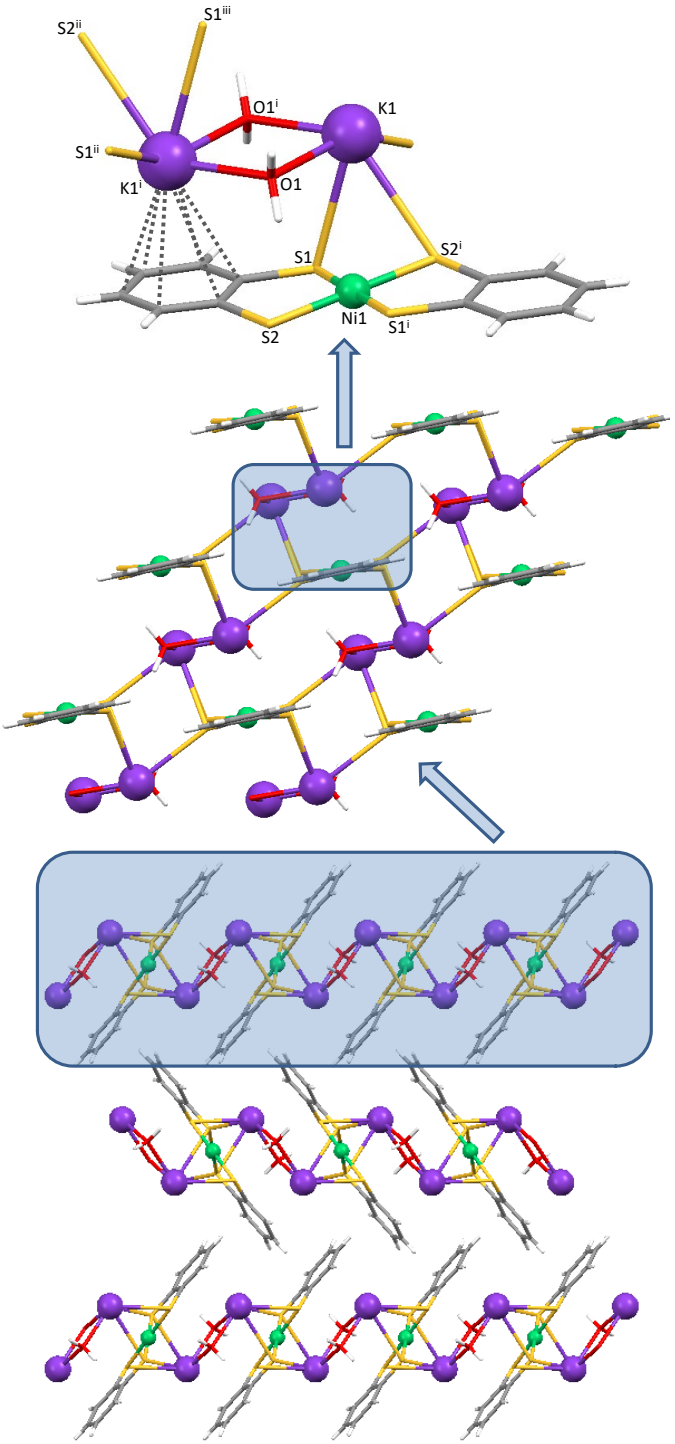

Figure 3. Coordination environment, 2D organometallic nature and lamellar supramolecular structure of compound **1**.

Similarly, compound **2** consists of $[Pd(SC_6H_4S)_2]^{2-}$ entities that behave as metalloligands towards K^+ cations but now the presence of THF molecules (Figure 2b), although retaining the bidimensional nature of the resulting metal-organic compound, modifies the way in which potassium atoms interact with the benzene-1,2-dithiolate ligands and as a consequence increase the complexity of the crystal structure. Table 3 collects selected bond lengths for **2**. Now, two palladium and three potassium metal centers can be crystallographically distinguished. The coordination environment of both palladium atoms is square planar (PdS_4) with two benzene-1,2-dithiolate ligands chelating the metal center through their thiolate groups. However, there is a distinctive shape difference between both $[Pd(SC_6H_4S)_2]^{2-}$entities: Pd2 is almost planar whereas Pd1 has a roof shape. The benzene-1,2-dithiolate ligands, although not coplanar, are arranged parallel around Pd2, although with a displacement of 0.68 Å, to provide a nearly planar entity, but the mean planes of the dithiolate ligands around Pd1 form a dihedral angle of 139° between them and 158/161° with respect to the PdS_4 core. As in **1**, the sulfur atoms of the benzene-1,2-dithiolate ligands are involved in two (1Pd + 1K) or three (1Pd + 2K) coordination bonds. The crystallographically independent potassium atoms form two different $[K_2(\mu\text{-}OH_2)_2]^{2+}$ entities: a symmetric one (K2-K2) and a non-symmetric one (K1-K3). The K2 atoms in the symmetric dimeric entity present a coordination sphere formed by two oxygen of the two bridging water molecules, one oxygen from one terminal THF molecule and three sulfur atoms from three palladium-dithiolenes. The potassium atoms (K1 and K3) in the non-symmetric dimeric entity present different coordination environments. K1 interacts with a η^6-benzene ring, two oxygens from two bridging water molecules and three sulfur atoms from two palladium dithiolene entities in a distorted octahedral geometry. K3 presents a similar coordination environment but includes an additional oxygen atom from a THF molecule that increases its coordination number up to

seven. This non-symmetric dimer creates a quite complex network of coordination bond connections, reinforced by O-H···S hydrogen bonds, that retains the 2D nature of the resulting structure (Figure 4).

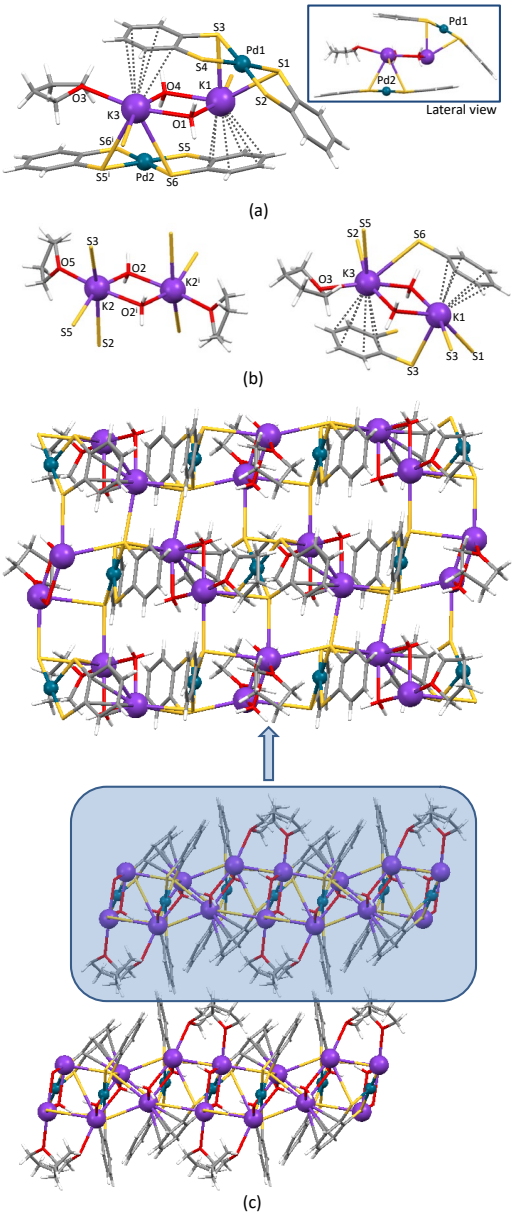

Figure 4. Details on the $[Pd(SC_6H_4S)_2]^{2-}$ (a) $[K_2(\mu\text{-}OH_2)_2]^{2+}$ (b) and entities present in compound **2**. (c) 2D metal-organic coordination polymer and crystal packing.

Table 3. Selected coordination bond lengths (Å) for compound **2**.

Pd1–S1	2.2965(13)	K1-O1	2.711(4)	K2-O2	2.709(4)	K3-O1^{iv}	2.735(4)
Pd1–S2	2.2946(13)	K1–O4	2.763(4)	K2-O2iii	2.793(5)	K3-O3	2.802(5)
Pd1-S3	2.3041(12)	K1–S1	3.2860(18)	K2-O5/K2-O5’	2.69(3)/2.73(4)	K3-O4^{iv}	2.682(4)
Pd1-S4	2.2986(12)	K1-S3	3.3057(17)	K2-S2	3.507(2)	K3-S2	3.2177(17)
Pd2-S5 x 2	2.2905(12)	K1-S3^{i}	3.2823(16)	K2-S3iii	3.4511(19)	K3-S5	3.5454(19)
Pd2-S6 x 2	2.2870(12)	K1-C13^{ii}	3.081(5)	K2-S4iii	3.7888(18)	K3-S6^{v}	3.5862(19)
		K1-C14^{ii}	3.194(5)	K2-S5	3.2733(16)	K3-C7^{iv}	3.960(6)
		K1-C15^{ii}	3.366(5)			K3-C8^{iv}	3.939(6)
		K1-C16^{ii}	3.432(5)			K3-C9^{iv}	3.501(6)
		K1-C17^{ii}	3.340(5)			K3-C10^{iv}	3.500(6)
		K1-C18^{ii}	3.153(5)			K3-C11^{iv}	3.519(6)
						K3-C12^{iv}	3.774(6)
Pd1···K1	3.4070(13)	Pd1···K2^{vi}	3.5534(14)	Pd2···K3	3.7176(14)	Pd2···K3^{v}	3.7176(14)

Symmetry codes: (i) –x, -y, -z+1; (ii) x-1, y-1, z; (iii) –x+1, -y+1, -z+1; (iv) –x+1, -y, -z+1; (v) –x+2, -y+1, -z+1; (vi) –x+1, -y+1, -z+1.

However, it substantially modifies the external surface, as now the THF molecules are also present avoiding the edge to face aromatic interactions observed for compound **1**. Therefore, the sheets are only held together by means of weak van der Waals interactions. As far as we know, compounds **1-2** are the first examples of alkali metal - group 10 metal dithiolene organometallic polymers.

The structure of compound $\{[K_2(\mu\text{-thf})_2][Pt(SC_6H_4S)_2]\}_n$ (**3**) consists of a 2D-CP (Figure 2c) in which the platinum centers in the $[Pt(SC_6H_4S)_2]^{2-}$ entities show a square planar coordination geometry as those observed for compounds **1** (Ni) and **2** (Pd). Table 4 collects the most relevant distances for compound **3**. The benzene-1,2-dithiolate ligands are nearly coplanar with a small dihedral angle of 4.6°. The lack of water molecules in the crystal structure forces the THF molecules to adopt the role of bridging ligands in the potassium dimeric entities, $[K_2(\mu\text{-THF})_2]^{2+}$. The distorted octahedral geometry around the potassium atoms is completed by the coordination of four sulfur atoms from two dithiolene entities without any evidence of η^6-coordination by the benzene groups. Both sulfur atoms of the benzene-1,2-dithiolate ligand are bonded to one platinum and two potassium metal centers. The $[Pt(SC_6H_4S)_2]^{2-}$ entities are perpendicular to the 2D coordination bond network with the benzene rings located at the external surface of the sheet in addition to the THF molecules. The latter avoids the presence of strong supramolecular interactions among the sheets that are only sustained by weak van der Waals interactions (Figure 5).

Table 4. Selected coordination bond lengths (Å) for compound **3**.

Pt1–S1 x 2	2.2984(17)	K1-O1 x 2	2.750(6)
Pt1–S2 x 2	2.2989(17)	K1–S1 x 2	3.343(3)
		K1–S2^{i} x 2	3.187(3)
		K2-O1^{ii} x 2	2.790(6)
		K2-S1 x 2	3.193(3)
		K2-S2^{ii} x 2	3.305(3)
Pt1···K1^{iii}	3.625(2)	Pt1···K2^{iv}	3.536(2)

Symmetry codes: (i) x+1/2, -y+1/2, -z+1/2; (ii) x, y, z-1; (iii) x-1/2, y, -z+1/2; (iv) x, y, z+1.

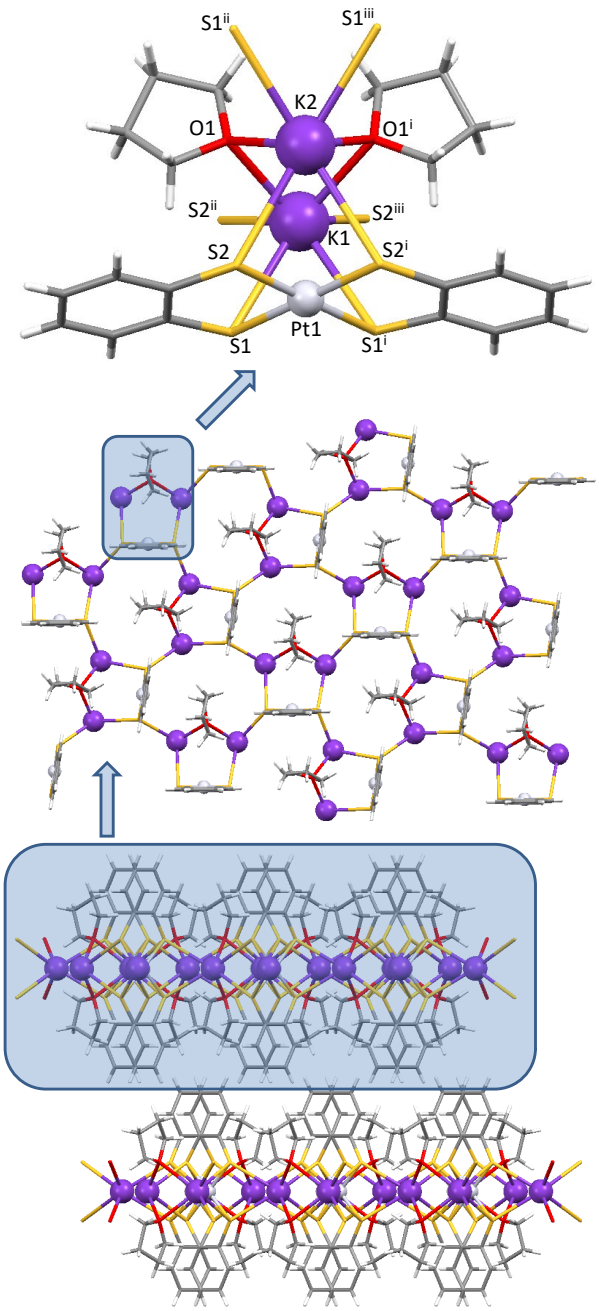

Figure 5. View of the coordination environments, representation of the 2D coordination polymer network and lamellar supramolecular structure of compound **3**.

The potassium coordination environments observed for these crystal structures are consistent with the theoretical predictions. Meanwhile in compounds **1** and **2**, the K atoms are located simultaneously on a C-ring hollow site and on a S-S bridge of the $[M(SC_6H_4S)_2]^{2-}$ units (in **2** the K2 atom coordinates to the sulfur atom completing its coordination environment with other oxygen donor ligands), for the Pt compound the K cations are located only on the S-S bridges, in agreement with the calculations that showed large $f^+(\boldsymbol{r})$ values on both S-S bridges. Albeit, given the equilibrium K-K distance within the crystals, the K atoms would not fit in this symmetric configuration because the K-K distance would be too short in the Ni compound, and too large in the Pd one. In contrast, $[Pt(SC_6H_4S)_2]^{2-}$ can nicely accommodate both K atoms on the two S-S bridges.

To further understand this interesting behavior, DFT-based calculations have been carried out using the two different configurations found in the $[M(SC_6H_4S)_2]^{2-}$ crystals (Figure S3). The result of these calculations reveal that the Ni (Figure S3a) and Pd (Figure S3b) compounds are more stable by 0.74 and 1.03 eV per unit cell in the configurations they adopt in the crystal. he Pt compound is also more stable by 0.61 eV per unit cell in the observed configuration (Figure S3c). Therefore, DFT-based calculations allow us to justify by both electronic and energetic considerations the packing configurations adopted by the building blocks within the different Ni, Pd and Pt crystals. Despite *a priori* one could consider that all the configurations could be similar for the three $[M(SC_6H_4S)_2]^{2-}$ entities, due to their similar electronic external configuration, slight differences in atomic size and orbital distribution in the metal atoms lead to form essentially different orbital hybridizations and change the packing arrangement from one compound to another.

Finally, the presence of the dithiolene complexes acting as metalloligands and the unusual structures found for **1**-**3**, prompted us to evaluate their fundamental electronic properties. Thus, magnetic susceptibility measurements confirmed their expected diamagnetic features.

Additionally, DC electrical conductivity measurements (Figures S5 and S6) showed that crystals of **1**-**3** are semiconductors with room temperature conductivities in the range 6×10^{-9} to 6×10^{-7} Scm^{-1} and activation energies *ca*. 710-740 meV (Table S1, Section S2 in ESI for experimental details). In all cases the similar electrical conductivities and activation energies can be attributed to the presence of similar pathways for the electron delocalization implying the M-dithiolene units, the K-S and K-O interactions. The complexity of the possible delocalization pathways

and the similarity of the conductivity values observed in the three samples, precludes any correlation between the structure and the electrical conductivity, which is evinced by the computed density of states profiles as a function of the energy for the Ni, Pd and Pt compounds (Figure S4) All three crystals exhibit a canonical wide band-gap behavior with energy gap values between the valence and conduction bands of 1.32, 1.65 and 2.27 eV for the Ni, Pd and Pt cases, respectively. These calculated large band-gaps agree with the experimental low conductivities measured and the high activation energies obtained. Interestingly, no significant morphological similarities are found between the three density of state profiles, indicating the lack of any correlation between the geometrical and electronic structure in these compounds, as aforementioned. Furthermore, we have observed that most crystals show a rapid degradation when they are submitted to low pressure and, therefore, the measured value might be lower that the real ones.

Conclusions

Theoretical calculations have been successfully used to predict coordination capabilities of the $[M(SC_6H_4S)_2]^{2-}$ (M = Ni, Pd or Pt) entities and evaluate their potential to produce novel organometallic polymers containing metalodithiolenes. These are the first examples of alkali metal - group 10 metal dithiolene organometallic polymers.

This work provides a clear example of the importance of theoretical tools for the structural design and the prediction of their physical properties.

Supporting Information. A pdf file with additional information on theoretical studies and physical properties is available free of charge. Files in CIF format for compounds **1-3** are (CCDC refs.: 1551942-1551944) available free of charge.

ACKNOWLEDGMENT

This work was supported in part by MICINN (grant MAT2016-77608-C3-1-P) and Generalitat Valenciana (PrometeoII/2014/076) and ISIC JIM acknowledges the financial support by the "Ramón y Cajal" Program of MINECO (RYC-2015-17730).

REFERENCES

(1) Eisenberg, R.; Gray, H. B. Noninnocence in Metal Complexes: A Dithiolene Dawn. *Inorg. Chem.* **2011***, 50*, 9741-9751.

(2) Pop, F.; Avarvari, N. Chiral Metal-Dithiolene Complexes. *Coord. Chem. Rev.* **2017***, 346*, 20-31.

(3) Robertson, N.; Cronin, L. Metal Bis-1,2-Dithiolene Complexes in Conducting Or Magnetic Crystalline Assemblies. *Coord. Chem. Rev.* **2002***, 227*, 93-127.

(4) Anonymous In *Dithiolene Chemistry: Synthesis, Properties and Applications;* Karlin, K. D., Stiefel, E. I., Eds.; Progress in Inorganic Chemistry; John Wiley & Sons, Inc.: New York, 2004; Vol. 52.

(5) Muller-Westerhoff, U. T.; Vance, B. In *Comprehensive coordination chemistry;* Wilkinson, G., Gillard, R. D. and McCleverty, J. A., Eds.; Pergamon Press: Oxford, U. K., 1987; Vol. 2.

(6) Clemenson, P. I. The Chemistry and Solid State Properties of Nickel, Palladium and Platinum Bis(Maleonitriledithiolate) Compounds. *Coord. Chem. Rev.* **1990***, 106*, 171-203.

(7) Ezzaher, S.; Gogoll, A.; Bruhn, C.; Ott, S. Directing Protonation in [FeFe] Hydrogenase Active Site Models by Modifications in their Second Coordination Sphere. *Chem. Commun.* **2010***, 46*, 5775-5777.

(8) Alcácer, L.; Novais, H. In: *Extended Linear Chain Compounds*; Miller, J. S., Ed.; Springer US; New York, 1983; Cap. 6, pp 319-351.

(9) Cassoux, P.; Valade, L.; Kobayashi, H.; Kobayashi, A.; Clark, R. A.; Underhill, A. E. Molecular Metals and Superconductors Derived from Metal Complexes of 1,3-dithiol-2-thione-4,5-dithiolate (Dmit). *Coord. Chem. Rev.* **1991***, 110*, 115-160.

(10) Sproules, S.; Wieghardt, K. O-Dithiolene and O-Aminothiolate Chemistry of Iron: Synthesis, Structure and Reactivity. *Coord. Chem. Rev.* **2010***, 254*, 1358-1382.

(11) Garreau de Bonneval, B.; Moineau-Chane Ching, K. I.; Alary, F.; Bui, T. T.; Valade, L. Neutral D8 Metal Bis-Dithiolene Complexes: Synthesis, Electronic Properties and Applications. *Coord. Chem. Rev.* **2010***, 254*, 1457-1467.

(12) Alvarez, S.; Vicente, R.; Hoffmann, R. Dimerization and Stacking in Transition-metal Bisdithiolenes and Tetrathiolates. *J. Am. Chem. Soc.* **1985***, 107*, 6253-6277.

(13) Takaishi, S.; Hosoda, M.; Kajiwara, T.; Miyasaka, H.; Yamashita, M.; Nakanishi, Y.; Kitagawa, Y.; Yamaguchi, K.; Kobayashi, A.; Kitagawa, H. Electroconductive Porous Coordination Polymer Cu[Cu(Pdt)2] Composed of Donor and Acceptor Building Units. *Inorg. Chem.* **2009***, 48*, 9048-9050.

(14) Ribas, X.; Dias, J. C.; Morgado, J.; Wusrt, K.; Santos, I. C.; Almeida, M.; Vidal-Gancedo, J.; Veciana, J.; Rovira, C. Alkaline Side-Coordination Strategy for the Design of Nickel(II) and Nickel(III) Bis(1,2-Diselenolene) Complex Based Materials. *Inorg. Chem.* **2004***, 43*, 3631-3641.

(15) Llusar, R.; Uriel, S.; Vicent, C.; Clemente-Juan, J.; Coronado, E.; Gómez-García, C. J.; Braïda, B.; Canadell, E. Single-Component Magnetic Conductors Based on Mo_3S_7 Trinuclear Clusters with Outer Dithiolate Ligands. *J. Am. Chem. Soc.* **2004***, 126*, 12076-12083.

(16) Llusar, R.; Triguero, S.; Polo, V.; Vicent, C.; Gómez-García, C. J.; Jeannin, O.; Fourmigué, M. Trinuclear Mo_3S_7 Clusters Coordinated to Dithiolate Or Diselenolate Ligands and their use in the Preparation of Magnetic Single Component Molecular Conductors. *Inorg. Chem.* **2008***, 47*, 9400-9409.

(17) Gushchin, A. L.; Llusar, R.; Vicent, C.; Abramov, P. A.; Gómez-Garcia, C. J. Mo_3Q_7 (Q = S, Se) Clusters Containing Dithiolate/Diselenolate Ligands: Synthesis, Structures, and their use as Precursors of Magnetic Single-Component Molecular Conductors. *Eur. J. Inorg. Chem.* **2013***, 2013*, 2615-2622.

(18) Machata, P.; Herich, P.; Luspai, K.; Bucinsky, L.; Soralova, S.; Breza, M.; Kozisek, J.; Rapta, P. Redox Reactions of Nickel, Copper, and Cobalt Complexes with "Noninnocent" Dithiolate Ligands: Combined in Situ Spectroelectrochemical and Theoretical Study. *Organometallics* **2014***, 33*, 4846-4859.

(19) Gao, X. K.; Dou, J. M.; Dong, F. Y.; Li, D. C.; Wang, D. Q. Synthesis, Crystal Structure and Electrochemical Properties of 2D Network Complex {[K(N18C6)]2(CH3CN)}[Ni(Mnt)2] with N18C6 = 2,3-Naphtho-18-Crown-6. *J. Inorg. Organomet. Polym. Mater.* **2004***, 14*, 227-237.

(20) Neves, A. I. S.; Santos, I. C.; Pereira, L. C. J.; Rovira, C.; Ruiz, E.; Belo, D.; Almeida, M. Ni-2,3-Thiophenedithiolate Anions in New Architectures: An in-Line Mixed-Valence Ni Dithiolene (Ni4–S12) Cluster. *Eur. J. Inorg. Chem.* **2011***, 2011*, 4807-4815.

(21) Dong, F. Y.; Dou, J. M.; Li, D. C.; Gao, X. K.; Wang, D. Q. Two-Dimensional Structural Topology Involving Pt/K and K/S Weak Interactions: Complex of Cis–anti–cis-Dicyclohexyl-18-Crown-6 with K2mnt and K_2PtCl_4. *J. Mol. Struct.* **2005***, 738*, 79-84.

(22) Gao, X. K.; Dou, J. M.; Li, D. C.; Dong, F. Y.; Wang, D. Q. Synthesis, Crystal Structure and Spectral Analysis of Crown Ether Platinum Bis(Dithiolate) Complexes $[Na(N15C5)_2]_2[Pt(Mnt)_2]$ and $[Na(N15C5)]_2[Pt(i\text{-}Mnt)_2]$. *J. Mol. Struct.* **2005***, 733*, 181-186.

(23) Gao, X. K.; Dou, J. M.; Li, D. C.; Dong, F. Y.; Wang, D. Q. Synthesis and Crystal Structures of Group 10 Metal Bis(Dithiolate) Complexes Constructed by 2,3-Naphtho-15-Crown-5 Or 2,3-Naphtho-18-Crown-6. *J. Incl. Phenom. Macrocycl. Chem.* **2005***, 53*, 111-119.

(24) Dong, F. Y.; Dou, J. M.; Li, D. C.; Gao, X. K.; Wang, D. Q. Synthesis, Characterization and Properties of One-Dimensional Complexes of Cis-Syn-Cis-Dicyclohexyl-18-Crown-6 with $K_2[M(Mnt)_2]$ (M=Ni, Pd, Pt). *J. Inorg. Organomet. Polym. Mater.* **2005***, 15*, 231-237.

(25) Sun, Y. M.; Dong, F. Y.; Dou, J. M.; Li, D. C.; Gao, X. K.; Wang, D. Q. Synthesis, Characterization and Thermogravimetric Analysis of Two Dicyclohexyl-18-Crown-6 Pd, Pt Isomaleonitriledithiolate Complexes. *J. Inorg. Organomet. Polym. Mater.* **2006***, 16*, 61-67.

(26) Long, D. L.; Cui, Y.; Chen, J. T.; Cheng, W. D.; Huang, J. S. One-Dimensional Coordination Polymers Formed by Crown Ether Metal Cation Bridges] Synthesis and Crystal Structure of Nickel(II) Dithiolene Complexes $[\{Na\text{-Benzo-15-Crown-5)}\}_2\ Ni(i\text{-}Mnt)_2]_n NCH_2Cl_2$ and $[\{Na\text{-Benzo-15-Crown-5)}\}_2\ Ni(i\text{-}Mnt)_2]_n$. *Polyhedron* **1998***, 17*, 3969-3975.

(27) Madalan, A. M.; Avarvari, N.; Fourmigué, M.; Clerac, R.; Chibotaru, L. F.; Clima, S.; Andruh, M. Heterospin Systems Constructed from $[Cu_2L_N]^{3+}$ and $[Ni(Mnt)_2]^{1-,2-}$ Tectons: First 3p-3d-4f Complexes (Mnt) Maleonitriledithiolato). *Inorg. Chem.* **2008***, 47*, 940-950.

(28) Kobayashi, Y.; Jacobs, B.; Allendorf, M. D.; Long, J. R. Conductivity, Doping, and Redox Chemistry of a Microporous Dithiolene-Based Metal-Organic Framework. *Chem. Mater.* **2010***, 22*, 4120-4122.

(29) Delgado, E.; Gómez-García, C. J.; Hernández, D.; Hernández, E.; Martín, A.; Zamora, F. Unprecedented Layered Coordination Polymers of Dithiolene Group 10 Metals: Magnetic and Electrical Properties. *Dalton Trans.* **2016***, 45*, 6696-6701.

(30) Smith, J. D. *Adv. Organomet. Chem.* **1999***, 43*, 267-348.

(31) Torvisco, A.; Decker, K.; Uhlig, F.; Ruhlandt-Senge, K. Heavy Alkali Metal Amides: Role of Secondary Interactions in Metal Stabilization. *Inorg. Chem.* **2009***, 48*, 11459-11465.

(32) Park, K. H.; Lee, K. M.; Go, M. J.; Choi, S. H.; Park, H. R.; Kim, Y.; Lee, J. New Class of Scorpionate: Tris(Tetrazolyl)−Iron Complex and its Different Coordination Modes for Alkali Metal Ions. *Inorg. Chem.* **2014***, 53*, 8213-8220.

(33) Baldamus, J.; Berghof, C.; Cole, M. L.; Evans, D. J.; Hey-Hawkins, E.; Junk, P. C. Attenuation of Reactivity by Product Solvation: Synthesis and Molecular Structure of [K{(η^6-Mes)NC(H)N(Mes)}{(η^6-Mes)- NHC(H)N(Mes)], the First Formamidinate Complex of Potassium. *Dalton Trans.* **2002**, 2802-2804.

(34) Yu, X. Y.; Jin, G. X.; Weng, L. H. Phenylthiolate as a s- and P- Donor Ligand: Synthesis of a 3-D Organometallic Coordination Polymer $[K_2Fe(SPh)_4]_N$. *Chem. Commun.* **2004**, 1542-1543.

(35) Bain, G. A.; Berry, J. F. Diamagnetic Corrections and Pascal's Constants. *J. Chem. Educ.* **2008***, 85*, 532-536.

(36) Farrugia, L. J. WinGX and ORTEP for Windows: An Update. *J. Appl. Cryst.* **2012***, 45*, 849-854.

(37) Sheldrick, G. M. A Short History of SHELX. *Acta Crystallogr.* **2008***, A64*, 112-122.

(38) Sheldrick, G. M. Crystal Structure Refinement with SHELXL. *Acta Crystallogr.* **2015***, C71*, 3-8.

(39) Sheldrick, G. M. Integrated Space-group and Crystal-structure Determination. *Acta Crystallogr.* **2015***, A71*, 3-8.

(40) Ayers, P. W.; Parr, R. G. Variational Principles for Describing Chemical Reactions: The Fukui Function and Chemical Hardness Revisited. *J. Am. Chem. Soc.* **2000***, 122*, 2010-2018.

(41) Ayers, P. W.; Morrison, R. C.; Roy, R. K. Variational Principles for Describing Chemical Reactions: Condensed Reactivity Indices. *J. Chem. Phys.* **2002***, 116*, 8731-8744.

(42) Gaussian 09, Revision **E.01**, Frisch, M. J.; Trucks, G. W.; Schlegel, H. B.; Scuseria, G. E.; Robb, M. A.; Cheeseman, J. R.; Scalmani, G.; Barone, V.; Mennucci, B.; Petersson, G. A.; Nakatsuji, H.; Caricato, M.; Li, X.; Hratchian, H. P.; Izmaylov, A. F.; Bloino, J.; Zheng, G.; Sonnenberg, J. L.; Hada, M.; Ehara, M.; Toyota, K.; Fukuda, R.; Hasegawa, J.; Ishida, M.; Nakajima, T.; Honda, Y.; Kitao, O.; Nakai, H.; Vreven, T.; Montgomery Jr., J. A.; Peralta, J. E.; Ogliaro, F.; Bearpark, M.; Heyd, J. J.; Brothers, E.; Kudin, K. N.; Staroverov, V. N.; Kobayashi, R.; Normand, J.; Raghavachari, K.; Rendell, A.; Burant, J. C.; Iyengar, S. S.; Tomasi, J.; Cossi, M.; Rega, N.; Millam, J. M.; Klene, M.; Knox, J. E.; Cross, J. B.; Bakken, V.; Adamo, C.; Jaramillo, J.; Gomperts, R.; Stratmann, R. E.; Yazyev, O.; Austin, A. J.; Cammi, R.; Pomelli, C.; Ochterski, J. W.; Martin, R. L.; Morokuma, K.; Zakrzewski, V. G.; Voth, G. A.; Salvador, P.; Dannenberg, J. J.; Dapprich, S.; Daniels, A. D.; Farkas, Ö.; Foresman, J. B.; Ortiz, J. V.; Cioslowski, J.; Fox, D. J., Gaussian, Inc., Wallingford CT (2009).

(43) Wang, H.; Butorin, S. M.; Young, A. T.; Guo, J. Nickel Oxidation States and Spin States of Bioinorganic Complexes from Nickel L-edge X-ray Absorption and Resonant Inelastic X-ray Scattering. *J. Phys. Chem. C* **2013***, 117*, 24767-24772.

(44) Giannozzi, P., Baroni, S.; Bonini, N.; Calandra, M.; Car, R.; Cavazzoni, C.; Ceresoli, D.; Chiarotti, G. L.; Cococcioni, M.; Dabo, I.; Corso, A. D.; de Gironcoli, S.; Fabris, S.; Fratesi, G.; Gebauer, R.; Gerstmann, U.; Gougoussis, C.; Kokalj, A.; Lazzeri, M.; Martin-Samos, L.; Marzari,

N.; Mauri, F.; Mazzarello, R.; Paolini, S.; Pasquarello, A.; Paulatto, L.; Sbraccia, C.; Scandolo, S.; Sclauzero, G.; Seitsonen, A. P.; Smogunov, A.; Umari, P.; Wentzcovitch, R. M., QUANTUM ESPRESSO: A Modular and Open-source Software Project for Quantum Simulations of Materials. *J. Phys. Condens. Matter* **2009***, 21*, 395502-395521.

(45) Perdew, J. P.; Burke, K.; Ernzerhof, M. Generalized Gradient Approximation made Simple. *Phys. Rev. Lett.* **1997***, 78*, 1396-1396.

(46) Rappe, A. M.; Rabe, K. M.; Kaxiras, E.; Joannopoulos, J. D. Optimized Pseudopotentials. *Phys. Rev. B* **1990***, 41*, 1227-1230.

(47) Monkhorst, H. J.; Pack, J. D. Special Points for Brillouin-Zone Integrations. *Phys. Rev. B* **1976***, 13*, 5188-5192.

(48) Barone, V.; Casarin, M.; Forrer, D.; Pavone, M.; Sambi, M.; Vittadini, A. Role and Effective Treatment of Dispersive Forces in Materials: Polyethylene and Graphite Crystals as Test Cases. *J. Comput. Chem.* **2009***, 30*, 934-939.

(49) Grimme, S. Semiempirical GGA-type Density Functional Constructed with a Long-range Dispersion Correction. *J. Comput. Chem.* **2006***, 27*, 1787-1799.

SYNOPSIS. Theoretical calculations allow to predict the coordination behavior of dithiolene $[M(SC_6H_4S)_2]^{2-}$ (M = Ni, Pd, Pt) as metalloligands giving rise to the isolation of organometallic polymers.